Bimodal Growth of Au on $SrTiO_3(001)$

Fabien Silly and Martin R. Castell

Department of Materials, University of Oxford, Parks Road, Oxford OX1 3PH, United Kingdom

(Received 12 August 2005; published 2 March 2006)

We have investigated the vapor phase growth of Au on $SrTiO_3(001)$-(2×1) substrates by UHV scanning tunneling microscopy. Submonolayer (ML) coverages below 300 °C wet the surface as disordered metastable 2D islands. Beyond 0.75 ML fcc nanocrystals with a (111) interface are nucleated and ripen by dewetting the surrounding layer. Some multiply twinned fivefold symmetric clusters are also created. Above 400 °C dewetting occurs for all coverages and the surface is only populated by nanocrystals and fivefold clusters. A planar ground state configuration for small Au clusters and a higher interface energy for crystals than for wetted 2D ML films explains these results.

DOI: 10.1103/PhysRevLett.96.086104 PACS numbers: 68.47.Jn, 68.37.Ef, 75.70.Kw

The behavior of gold nanoparticles is of significant interest because of their unique optical and chemical properties. Bulk gold tends to be inert, but in its nanoparticle form it can act as a highly efficient catalyst. For example, Au clusters and thin films supported on titana have unusual catalytic properties [1–4] when one dimension of the cluster becomes smaller than 3 atomic spacings [1,3,5]. The optical behavior of gold is also interesting. Surface plasmon resonances [6–8] can be tuned through size selection of nanoparticles. Supported self-assembled gold nanocrystal assemblies with specific shapes and sizes are therefore a focus of research in connection with applications in nano-optics and optical sensor technologies. Thus it is critical to develop a fundamental understanding of the atomic-scale processes that underlie thin film and nanocrystal growth, and establish their influence on film morphology or crystal shape. In turn, this will enable control over the properties of Au nanostructures and allow them to be tailored for specific applications. The substrate used in our studies is $SrTiO_3$, which is used for the growth of high T_c cuprate superconductors [9,10] and metal [11,12] or semiconductor thin films. $SrTiO_3$ crystallizes into the cubic perovskite structure with a 3.905 Å lattice parameter and has a multitude of different reconstructions depending on sample preparation [13,14].

In this Letter we report on a study of Au grown on (2×1) reconstructed $SrTiO_3(001)$ crystal surfaces. This system displays interesting and unexpected behavior in that two growth modes are observed, also called bimodal growth. Au either wets the surface or forms nanocrystals. Wetted areas can transform to nanocrystals, but they do so by a dewetting process. This unusual behavior does not fall into the normal categories of metal on oxide crystal growth.

In its pure form $SrTiO_3$ has a 3.2 eV band gap which makes it too insulating for STM imaging, and we therefore use Nb doped (0.5% weight) $SrTiO_3$. The $SrTiO_3$ crystals were epipolished (001) and supplied by PI-KEM, UK. We deposited Au from an *e*-beam evaporator (Oxford Applied Research EGN4) using 99.95% pure Au rods supplied by Goodfellow, UK. Our STM is manufactured by JEOL (JSTM 4500 s) and operates in UHV (10^{-8} Pa). We used etched *W* tips to image the samples at room temperature with a bias voltage applied to the sample. The $SrTiO_3$ samples were sputtered with argon ions and subsequently annealed in UHV at 600 °C for 9 h. The (2×1) surface reconstruction was imaged by STM and confirmed by low energy electron diffraction. This reconstruction has been investigated previously in detail by STM and LEED [13], and the structure has been solved by transmission electron diffraction [15].

Figure 1 shows STM images of Au on $SrTiO_3$ with increasing coverage. The substrate temperature during deposition was 210 °C. In Fig. 1(a) 0.25 monolayers (ML) of Au were deposited, which wet the surface resulting in flat islands with irregular edges and is reminiscent of strict layer-by-layer growth (Frank–van Der Marwe growth). In this Letter 1 ML is the equivalent surface density of Au that is required to form a complete surface wetting layer. The coverage has been increased to 0.75 ML for Fig. 1(b) causing the flat islands to grow and almost cover the substrate surface. Additionally, some crystals with increased height and straight edges can be seen in the image. These crystals most likely nucleated in the wetted monolayer, and grew rapidly by dewetting the immediate Au around them. This process is not cluster evolution on top of a wetting layer (Stranski-Krastanov growth) because the nanocrystal consumes the wetting layer, and the crystallography of the interface is changed. The result is that the substrate around the immediate vicinity of the nanocrystals is exposed, so that for a 1.25 ML deposition more substrate is exposed than for a 0.75 ML deposition. This has the same end result as direct island growth on the surface (Vollmer-Weber growth). In Fig. 1(c) the Au coverage has been increased to 1.25 ML. The density of regular crystals is now significantly higher. With further Au deposition to 1.5 ML [Fig. 1(d)] the nanocrystals dominate the surface. The STM images in Figs. 1(c) and 1(d) reveal that most of the Au nanocrystals have a truncated triangle top surface parallel to the substrate with 6 side facets, which we term hexagons. In addition, detailed study of the images shows that there are also a minority of icosahedral nanocrystal shapes. We

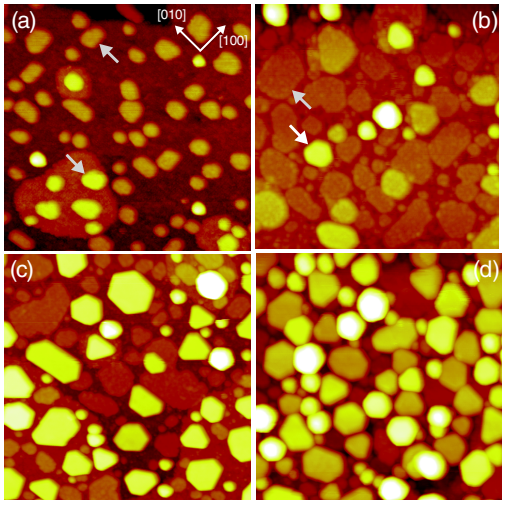

FIG. 1 (color online). STM images (80×80 nm^2) of Au deposited onto a 210 °C $SrTiO_3(001)$-(2×1) substrate. (a) A 0.25 ML deposition results in around 60 wetted 2D islands, of which two typical examples are indicated by gray arrows. $V_s = +1.0$ V, $I_t = 50$ pA. (b) A 0.75 ML deposition causes the 2D islands to increase in size (gray arrow) and the nanocrystals to be nucleated (white arrow). $V_s = +2.0$ V, $I_t = 50$ pA. (c) As the coverage is increased to 1.25 ML more nanocrystals are nucleated. $V_s = +2.0$ V, $I_t = 50$ pA. (d) At 1.5 ML coverage the surface is almost exclusively covered in nanocrystals. $V_s = +2.0$ V, $I_t = 50$ pA.

will now examine in turn layer growth, hexagon nanocrystals, and icosahedral cluster shapes.

Figure 2(a) shows a STM image of 0.1 ML of Au deposited on a $SrTiO_3$ substrate heated to 300 °C. The same flat islands as shown in Fig. 1(a) are seen in this image, which was taken at a sample bias of +1.5 V. Figure 2(b) is of the same area as Fig. 2(a), but now the sample bias was set to +2.5 V and the Au islands are no longer discernible above the substrate background. We find that for lower sample biases, the island heights appear higher. Specifically, for biases of +1.0, +1.5, and +2.5 V, the island heights are measured as ~7, ~4, and ~0 Å, respectively. For sample biases above +2.5 V the Au islands appear as depressions, so that, for example, a +4 V bias results in island "heights" of −4 Å. These dramatic changes of apparent height with sample bias point to a significant difference in the relative surface local density of states (LDOS) for the Au monolayer and the $SrTiO_3$ substrate. This is because the tunneling current in the STM is proportional to the LDOS as well as the tip-sample separation. The measured step height from the $SrTiO_3(001)$ terrace to the Au monolayer is therefore a function of the physical height and the relative LDOS of the substrate and island. By changing sample bias we access different parts of the LDOS energy spectrum, which in turn influences the step height measurement. It should be noted that for a given sample bias we only ever observe a single island height indicating that the flat islands are monolayers of Au.

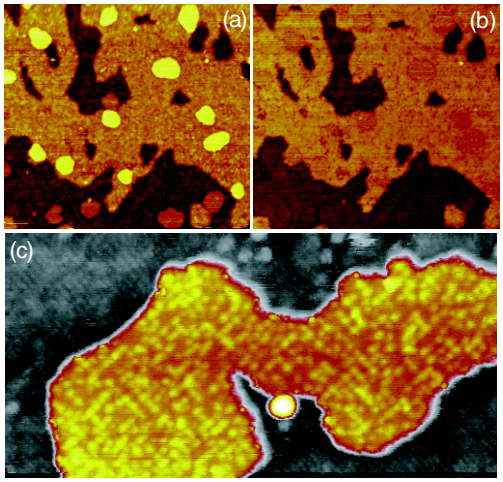

FIG. 2 (color online). Submonolayer deposition of Au onto a 300 °C $SrTiO_3(001)$-(2×1) substrate gives rise to monolayer islands. The STM images in (a) and (b) are of the same area (170×155 nm^2), but with different sample biases. The 17 Au islands in (a) ($V_s = +1.5$ V, $I_t = 50$ pA) cannot be seen at the higher bias in (b) ($V_s = +2.5$ V, $I_t = 50$ pA). Panel (c) shows a high resolution image of the Au monolayer island surface. Moiré structures can be seen on the island, and the (2×1) substrate reconstruction is visible surrounding it (60×30 nm^2); ($V_s = +0.8$ V, $I_t = 0.3$ nA).

The crystallographic relationship between the Au islands and the substrate can be derived from the high resolution image in Fig. 2(c). The surface around the island shows the characteristic (2×1) reconstruction of the $SrTiO_3(001)$ substrate. It is worth noting that the surface does not restructure due to Au deposition for any of our Au on $SrTiO_3(001)$ experiments. The Au island itself has irregular edges. However, bright spots appear in the image that have a periodicity of 10.3 Å and run in rows along the [010] and [100] directions of the $SrTiO_3(001)$ substrate. This indicates that there is a degree of frustrated commensurate epitaxy between the Au monolayer and the substrate that results in a moiré interaction which gives rise to the periodic arrangement of bright spots. The inhomogeneous moiré pattern reflects the irregularity of the Au monolayer. We can dismiss the possibility that the wetting layer is due to adsorption of Au atoms on surface defects because the defect density on the (2×1) surface is too low [13] for this to occur. Defect sites may however act as nucleation centers for the growth of the wetting layer islands.

We now turn to the alternative growth behavior for Au on $SrTiO_3$, which is nanocrystal formation. As demonstrated in Fig. 1, nanocrystals are nucleated when the amount of Au deposited exceeds ~0.75 ML. However, we find that nanocrystals can also be created through higher substrate temperatures either during deposition or in a postdeposition anneal. Figure 3(a) shows the topography of the $SrTiO_3(001)$-(2×1) surface following 0.8 ML of Au deposited onto a substrate heated to 400 °C. Only nanocrystals and no monolayer islands are seen in this temperature range. The nanocrystals have truncated tri-

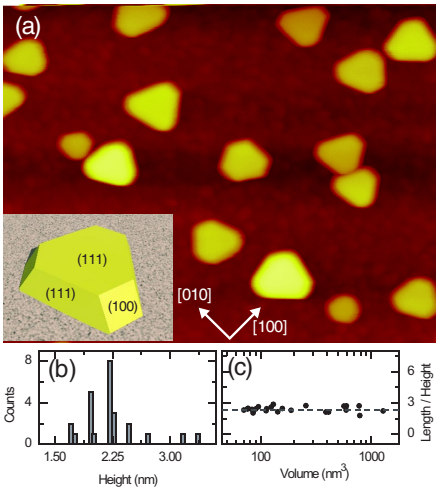

FIG. 3 (color online). (a) Au deposition onto a 400 °C substrate gives rise to truncated triangle shaped nanocrystals only (100×78 nm^2); ($V_s = +2.0$ V, $I_t = 0.1$ nA). Inset: truncated triangle shape, the {111} and {001} faces are indicated. (b) A histogram shows the distribution of nanocrystal heights. (c) Shows that the ratio of nanocrystal length to height is constant as a function of cluster volume.

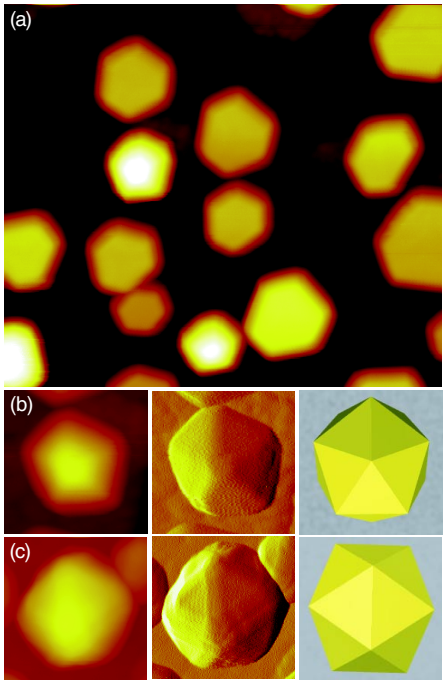

FIG. 4 (color online). (a) Au deposition onto a 210 °C $SrTiO_3(001)$-(2×1) substrate followed by a 500 °C anneal (12 h) gives rise to single crystal Au islands (hexagon shape) and multiple twinned particles (pentagon shape) (80×70 nm^2); $V_s = +2.5$ V, $I_t = 50$ pA. Au icosahedron, point orientation (b) (18×18 nm^2) and edge orientation (c) (24×24 nm^2), topography, derivative image, and model. ($V_s = +2.0$ V, $I_t = 50$ pA).

angle top facets and bases, with three small side facets and three large side facets. This shape corresponds to a supported face centered cubic (fcc) crystal with a (111) top facet, three large (111) side facets, and three small (001) side facets. There is a distinct height quantization of these nanocrystals [Fig. 3(b)] into steps of around 2.4 Å, which corresponds to the Au (111) interplanar spacing of 2.35 Å, as expected.

The nanocrystals of Fig. 3(a) have two preferred epitaxial orientations. The Au interface is always a (111) plane, but one of the edge facets can be parallel to either the $\langle 110 \rangle$ or $\langle 100 \rangle$ $SrTiO_3$ directions. Formally, these epitaxial relationships are expressed as $(111)_{Au} \| (001)_{SrTiO_3}$, $[110]_{Au} \| [110]_{SrTiO_3}$ and $(111)_{Au} \| (001)_{SrTiO_3}$, $[110]_{Au} \| [100]_{SrTiO_3}$. Figure 3(c) shows the length-to-height ratio as a function of volume. The length in this instance is the width across the top of the hexagon from the middle of one (001) side facet to the middle of the opposite (111) side facet. The ratio of $l/h = 2.39 \pm 0.26$ is constant with volume, which implies that these nanocrystals have reached their equilibrium shape.

As mentioned previously, when Au nanocrystals form there is a minority that adopt an icosahedral shape. Figure 4(a) shows an image of 1.5 ML deposited at 210 °C and subsequently annealed at 500 °C for 12 h. Dewetting of the monolayer islands occurs during this post anneal. Of the 12 nanocrystals in the image 10 are of the familiar hexagon shape, and two have pentagonal symmetry. These types of crystals are know to evolve from multiple twinning, which allows only (111) facets to be exposed and can therefore be a low energy shape as long as the energy of the twin boundaries are sufficiently low.

Figs. 4(b) and 4(c) show in detail images and models of icosahedrons with (b) point orientation and (c) edge orientation. Icosahedral nanocrystals have been observed by electron microscopy [16], but we believe that these are the first reports of STM images of these shapes.

The most surprising aspect of the experimental work are the two distinct growth modes of Au. Monolayer wetting of the surface requires that $\gamma_{STO} > \gamma_{Au} + \gamma_i$, where γ_{STO} is the surface energy of the $SrTiO_3$ substrate, γ_{Au} is the monolayer surface energy, and γ_i is the interface energy between the monolayer and the substrate. However, for nanocrystal growth with no wetting layer this inequality is reversed. How then is it possible to reconcile both growth modes for the same metal on oxide system? In great part the answer must lie in the interface energy γ_i, which will be different for ML wetting and nanocrystal growth, because the former has a disordered interface and the latter a single crystal interface. The Au surface energies will also be different for the two growth modes. This results in the following inequality:

$$\gamma_{AuC} + \gamma_{iC} - \gamma_{STO} > 0 > \gamma_{AuML} + \gamma_{iML} - \gamma_{STO}, \quad (1)$$

where the C subscript refers to crystalline growth. We can estimate $\gamma_{STO} = (2.5 \pm 0.5)$ J/m^2 from *ab initio* calculations [17] of the (2×1) reconstruction. Furthermore, we can derive $\gamma_C^* = \gamma_{iC} - \gamma_{STO}$ through a straightforward

analysis of the nanocrystal geometry via the modified Wulff construction [18]:

$$\gamma_C^* = \sqrt{\frac{3}{2}}\gamma_{001}\left(\frac{l}{h}\right)^{-1} - \gamma_{111}, \quad (2)$$

where $l/h = 2.39 \pm 0.26$ is the height to length ratio of the nanocrystals determined experimentally [Fig. 3(c)], and γ_{111} and γ_{001} are the theoretically determined surface facet energies of Au taken from Vitos *et al.* [19]: $\gamma_{001} = 1.627\ \mathrm{J/m^2}$, $\gamma_{111} = 1.283\ \mathrm{J/m^2}$. This results in $\gamma_C^* = (-0.45 \pm 0.09)\ \mathrm{J/m^2}$. We can therefore determine γ_{iC} as being $(2.05 \pm 0.51)\ \mathrm{J/m^2}$, which is a relatively large interface energy. Conversely, the interface energy for $\gamma_{i\mathrm{ML}}$ must be below $1.22 \pm 0.5\ \mathrm{J/m^2}$ for wetting to occur. We can therefore conclude that the difference in interface energy for nanocrystals and wetted monolayers is at least $0.83\ \mathrm{J/m^2}$. We can, in addition, calculate the adhesion energy γ_{adh} of the Au nanocrystals with a (111) interface on $SrTiO_3(001)$-(2×1), which is defined by: $\gamma_{\mathrm{adh}} = \gamma_{111} - \gamma_{iC} + \gamma_{\mathrm{STO}} = \gamma_{111} - \gamma_C^*$. This results in $\gamma_{\mathrm{adh}} = (1.732 \pm 0.091)\ \mathrm{J/m^2}$.

The explanation for the bimodal growth of Au on $SrTiO_3(001)$ can thus be explained in the following manner. Au islands nucleate as monolayer wetted structures because small Au clusters have a planar ground state configuration [20]. The planar Au nanoclusters grow into wetted monolayers when incoming atoms attach to the sides of the islands, and the monolayer islands readily wet the surface because they have a low interface energy. Presumably the low interface energy arises because the Au monolayer is not constrained by an atomic layer above it, which allows a degree of layer relaxation and hence some local commensurate epitaxy. Beyond a certain size the wetted islands become metastable. They are no longer the lowest energy configuration and the thermodynamically stable structure is a 3D nanocrystal. But for the transition from a wetted layer to a nanocrystal to occur a 3D crystal shape of a minimum size needs to be nucleated. There is no smooth transition from wetting to nanocrystal formation because layer-by- layer growth (Frank–van Der Marwe growth) is energetically unfavorable beyond the first monolayer. This means that there is a barrier due to the increased interface energy of the nanocrystals that needs to be overcome in order to move from wetting to nanocrystal formation. This occurs if enough Au atoms act cooperatively and are hence able to nucleate a nanocrystal. Nanocrystal nucleation can either be forced by deposition of more Au on top of an established ML, or by providing sufficient thermal energy. Once nucleated, the nanocrystals ripen by dewetting the Au in their immediate vicinity.

The behavior reported here can be compared with studies of Au on $TiO_2(110)$ by Zhang *et al.* [21], which can also be explained through bimodal growth. Other studies of Au on $TiO_2(110)$ have reported either only nanocluster growth [22] or only wetting [23], but these studies are also consistent given the variety of temperatures and amount deposited. A model for the growth of Au on TiO_2 has been proposed by Parker *et al.* [24], which we believe is also applicable to the Au on $SrTiO_3(001)$ system, except that we observe the additional step of a dewetting process during the ML to nanocrystal transformation.

In summary, we have investigated Au bimodal growth on a $SrTiO_3(001)$-(2×1) support. Our results show that Au can form metastable monolayer 2D wetted islands at low temperatures and low Au coverages, or upon increased Au deposition give rise to fcc nanocrystals and icosahedral multiply twinned particles with associated dewetting. These particles and nanocrystals can alternatively form directly at high temperatures even for low Au concentrations. For Au on $SrTiO_3(001)$-(2×1) we have obtained a value of the adhesion energy $\gamma_{\mathrm{adh}} = (1.732 \pm 0.091)\ \mathrm{J/m^2}$. We have also estimated that the fcc nanocrystal interface energy is at least $0.83\ \mathrm{J/m^2}$ greater than for wetted Au monolayers. Given the intense interest in Au catalysts on titanate supports, we believe our results will significantly aid the understanding necessary to optimize the processing conditions for these new catalytic and sensing systems.

The authors would like to thank the Royal Society and DSTL for funding, and Chris Spencer (JEOL UK) and Doug Imeson (DSTL) for valuable support.

[1] M. S. Chen and D. W. Goodman, Science **306**, 252 (2004).
[2] A. T. Bell, Science **299**, 1688 (2003).
[3] M. Valden, X. Lai, and D. W. Goodman, Science **281**, 1647 (1998).
[4] N. Lopez *et al.*, J. Catal. **223**, 232 (2004).
[5] M. Valden *et al.*, Catal. Lett. **56**, 7 (1998).
[6] D. M. Schaadt *et al.*, Appl. Phys. Lett. **86**, 063106 (2005).
[7] G. Laurent *et al.*, Nano Lett. **5**, 253 (2005).
[8] C. Sonnichsen and A. P. Alivisatos, Nano Lett. **5**, 301 (2005).
[9] J. Padilla and D. Vanderbilt, Surf. Sci. **418**, 64 (1998).
[10] P. J. Moller *et al.*, Surf. Sci. **425**, 15 (1999).
[11] F. Silly and M. R. Castell, Phys. Rev. Lett. **94**, 046103 (2005).
[12] T. Wagner *et al.*, J. Appl. Phys. **89**, 2606 (2001).
[13] M. R. Castell, Surf. Sci. **505**, 1 (2002).
[14] T. Kubo and H. Nozoye, Surf. Sci. **542**, 177 (2003).
[15] N. Erdman *et al.*, Nature (London) **419**, 55 (2002).
[16] L. D. Marks, Rep. Prog. Phys. **57**, 603 (1994).
[17] K. Johnston *et al.*, Phys. Rev. B **70**, 085415 (2004).
[18] W. L. Winterbottom, Acta Metall. **15**, 303 (1967).
[19] L. Vitos *et al.*, Surf. Sci. **411**, 186 (1998).
[20] H. Hakkinen *et al.*, Angew. Chem.. Int. Ed. **42**, 1297 (2003).
[21] L. Zhang *et al.*, Phys. Rev. B **56**, 10 549 (1997).
[22] C. E. J. Mitchell *et al.*, Surf. Sci. **490**, 196 (2001).
[23] Q. L. Guo *et al.*, Surf. Interface Anal. **32**, 161 (2001).
[24] S. C. Parker *et al.*, Surf. Sci. **441**, 10 (1999).